Vol. 647: 49–64, 2020
https://doi.org/10.3354/meps13390

MARINE ECOLOGY PROGRESS SERIES
Mar Ecol Prog Ser

Published August 13

Ocean acidification impacts on biomass and fatty acid composition of a post-bloom marine plankton community

Isabel Dörner[1], Helena Hauss[1,*], Nicole Aberle[2], Kai Lohbeck[1,3], Carsten Spisla[1], Ulf Riebesell[1], Stefanie M. H. Ismar-Rebitz[1]

[1]GEOMAR Helmholtz Center for Ocean Research Kiel, 24105 Kiel, Germany
[2]Trondhjem Biological Station, Department of Biology, Norwegian University of Science and Technology (NTNU), 7491 Trondheim, Norway
[3]*Present address:* Limnological Institute, University of Konstanz, 78464 Konstanz, Germany

ABSTRACT: A mesocosm approach was used to investigate the effects of ocean acidification (OA) on a natural plankton community in coastal waters off Norway by manipulating CO_2 partial pressure (pCO_2). Eight enclosures were deployed in the Raunefjord near Bergen. Treatment levels were ambient (~320 µatm) and elevated pCO_2 (~2000 µatm), each in 4 replicate enclosures. The experiment lasted for 53 d in May–June 2015. To assess impacts of OA on the plankton community, phytoplankton and protozooplankton biomass and total seston fatty acid content were analyzed. In both treatments, the plankton community was dominated by the dinoflagellate *Ceratium longipes*. In the elevated pCO_2 treatment, however, biomass of this species as well as that of other dinoflagellates was strongly negatively affected. At the end of the experiment, total dinoflagellate biomass was 4-fold higher in the control group than under elevated pCO_2 conditions. In a size comparison of *C. longipes*, cell size in the high pCO_2 treatment was significantly larger. The ratio of polyunsaturated fatty acids to saturated fatty acids of seston decreased at high pCO_2. In particular, the concentration of docosahexaenoic acid (C 22:6*n*3c), essential for development and reproduction of metazoans, was less than half at high pCO_2 compared to ambient pCO_2. Thus, elevated pCO_2 led to a deterioration in the quality and quantity of food in a natural plankton community, with potential consequences for the transfer of matter and energy to higher trophic levels

KEY WORDS: Microphytoplankton · Microzooplankton · pH · Lipids · Mesocosm · Food quality · *Ceratium*

1. INTRODUCTION

The atmospheric CO_2 concentration has been rising since the industrial revolution, and is one of the major factors driving global warming via the greenhouse effect (IPCC 2017). The ocean is a net CO_2 sink, annually taking up approximately one-third of anthropogenic CO_2 emissions, thereby slowing down global warming (Le Quéré et al. 2016 and references therein). While dissolved CO_2 is a potential limiting resource for autotrophic organisms, it is potentially harmful due to its capacity to increase H^+ concentrations (reduce pH) and result in ocean acidification (OA). Hence, OA is one of the main consequences of ongoing global change in the marine environment (along with warming and ocean deoxygenation). Global mean atmospheric values of the partial pressure of CO_2 (pCO_2) have increased from pre-industrial values of <300 to >400 µatm today, and the average surface ocean pH has already dropped by

*Corresponding author: hhauss@geomar.de

~0.1 units (Fabry et al. 2008) and could drop by 0.15–0.2 units over the next centuries even if carbon emission reduction efforts to limit global warming to 2°C are successful (IPCC 2017). While projections for global atmospheric mean values of pCO_2 for 2100 differ between 450 and 1000 µatm depending on our CO_2 reduction efforts, local marine conditions in coastal regions are already more extreme with values >3000 µatm for restricted time periods (Melzner et al. 2013); thus up to 4000 µatm is a realistic scenario for coastal ecosystems.

Marine phytoplankton fixes about 50 Gt of carbon yr^{-1} (Field et al. 1998), which is approximately half of global net primary production. It forms the basis of the oceanic food web, providing nourishment to higher trophic levels thus stimulating secondary production. In turn, micro- and mesozooplankton standing stocks support growth and condition of commercially important fish species (Harvey et al. 2012). OA effects on phytoplankton biomass, community composition and elemental composition can thus indirectly affect the growth and reproduction of secondary and tertiary consumers (Andersson et al. 2003, Malzahn et al. 2007, 2010, Rossoll et al. 2012). Thus, OA effects on marine primary and secondary producers may translate to higher trophic levels and ultimately alter ecosystem services, including fishery yields. As phytoplankton plays such an important role as the base of marine food webs, the consequences of OA on these organisms are of acute interest. Influences of OA could impact natural plankton communities in several ways. First, the individual organisms could be directly affected by OA, leading to changes in their biochemistry, overall growth rate or biomass production (Riebesell et al. 2017). Second, food quality could be influenced by different elemental compositions (i.e. cellular C:N or C:P ratios) or changes in fatty acid (FA) compositions (Tsuzuki et al. 1990, Rossoll et al. 2012). On the other hand, OA could influence the composition of the phytoplankton community, which could indirectly trigger changes in food quality measures or biomass production. In this context, protozooplankton, acting both as a primary grazer of phytoplankton and as a trophic intermediary between primary producers and secondary consumers (e.g. copepods and larval fish), play a pivotal role (Calbet 2008, Calbet et al. 2014). Further, protozooplankton is considered to improve the food quality for higher trophic levels by buffering nutritional imbalances at the interface between primary production and consumption, a pattern described as 'trophic upgrading' (Gifford 1991, Klein Breteler et al. 1999).

Changes in the phytoplankton community (including e.g. size distribution, ballasting structures) may also influence the efficiency of the ocean to act as a sink by exporting carbon from the surface layers to the deep ocean (Tortell et al. 2008). While species with calcium carbonate shells are thought to be negatively affected by OA (Meyer & Riebesell 2015), others, such as diatoms, may benefit from decreased ocean pH due to a stimulation of growth at high CO_2 levels (e.g. Tortell et al. 2008, Trimborn et al. 2013). Species-specific beneficial effects of increased CO_2 are due to direct fertilization by CO_2, which benefits specific algal taxa according to their relative efficiency in carbon-concentrating mechanisms (CCMs) (Giordano et al. 2005). However, OA does not generally enhance growth in diatoms. In the same study that showed positive effects of OA on *Chaetoceros debilis*, other diatom species remained unaffected by OA (Tortell et al. 2008). Former studies on (natural) phytoplankton communities focusing on diatoms also identified OA-sensitive and OA-insensitive species (Kim et al. 2006, Tatters et al. 2013).

In mesocosm community approaches, effects on the succession and composition of phytoplankton were also ambiguous, with no effects (Riebesell et al. 2007), positive effects e.g. for picophytoplankton (Schulz et al. 2017), negative effects by stimulating toxic phytoplankton blooms (Riebesell et al. 2018) and/or differences in community composition (Grossart et al. 2006, Tortell et al. 2008, Schulz et al. 2013, Alvarez-Fernandez et al. 2018). Even in cases where phytoplankton composition appeared unaffected, phytoplankton cells were influenced by OA. Such effects included e.g. increased biological carbon consumption due to enhanced photosynthesis (Riebesell et al. 2007, Eberlein et al. 2017) or a shift in nutrient flux into different phytoplankton groups at high pCO_2 (Schulz et al. 2013).

The quality of phytoplankton standing stocks is important for higher trophic levels because metazoans are not able to synthesize all required compounds (such as certain amino acids, FAs or vitamins) de novo themselves. Instead, essential nutrients must be taken up from the food source (autotrophic or heterotrophic protists). One aspect of the food quality of protists (phyto- and protozooplankton) is their FA composition (Dalsgaard et al. 2003). Some polyunsaturated fatty acids (PUFAs) are essential for the development and reproduction of metazoans (Sargent & Falk-Petersen 1988, Bell et al. 2007). Docosahexaenoic acid (DHA; 22:6*n*3) and eicosapentaenoic

acid (EPA; C 20:5*n*3c) are of particular importance for growth and reproduction in copepods (Støttrup & Jensen 1990, Arendt et al. 2005, Rossoll et al. 2012).

Studies investigating the effect of OA on FA content/composition of phytoplankton have found diverse responses to elevated pCO_2 for different species and groups (Riebesell et al. 2000, Wynn-Edwards et al. 2014, Bermúdez et al. 2015, Bi et al. 2017, 2018). As an example, OA was shown to affect the FA content/composition in the diatom *Thalassiosira pseudonana* (Rossoll et al. 2012). In that study, elevated pCO_2 resulted in changes in growth and reproduction in the copepod *Acartia tonsa*, leading to slower stage development and decreased egg production, resulting in lower trophic transfer efficiency. Thus, indirect effects of OA through trophic transfer are possible and there is an urgent need to consider OA impacts using natural plankton communities (Leu et al. 2013, J. R. Bermúdez et al. 2016, R. Bermúdez et al. 2016).

In this study, we investigated the influence of OA on the community composition of planktonic protists (phyto- and protozooplankton) and assessed the impact of food quantity and quality of protists in altering trophic transfer efficiency and the condition of higher trophic levels. Our study was thus tailored to address the question whether direct OA impacts, as shown in monoculture experiments, play out in natural plankton communities or whether they are alleviated by community composition changes.

2. MATERIALS AND METHODS

2.1. Experimental setup

The study described here was conducted in early summer in Raunefjorden, Norway, using the Kiel Off-Shore Mesocosms for Future Ocean Simulations (KOSMOS) large-scale infrastructure (Riebesell et al. 2013). Raunefjorden is a 15 km long, 4 km wide fjord on the west coast of Norway, close to the city of Bergen, with a surface salinity around 30 (Molvær et al. 2007). Water depth at the mesocosm deployment site (60° 15′ 55″ N, 5° 12′ 21″ E) ranged from 50–75 m.

In total, 8 KOSMOS mesocosms were deployed; these were 2 m in diameter and 21 m in length and enclosed around 60 m^3 of water. The mesocosms were open at the top but equipped with a roof to minimize precipitation into the enclosures. The experiment was run over a duration of 53 d (9 May–30 June 2015). To alter CO_2 conditions with minimal disturbance to the enclosed community, seawater carbonate chemistry was manipulated through addition of CO_2-enriched fjord water (Riebesell et al. 2013). We applied 2 different treatment levels with 4 replicates each: an ambient pCO_2 level, where no CO_2 was added artificially (initial values were around 270 µatm) and an elevated pCO_2 level with a target value of 2000 µatm. The high pCO_2 treatment was about 2 times higher than projected for 2100 (IPCC 2017), bearing in mind that coastal systems are prone to larger variability and locally increased pCO_2 values (Melzner et al. 2013).

The start of the experimental manipulation (CO_2 addition) was defined as t_0. Mesocosms were closed at the bottom 5 d before (t_{-5}) and sampling was started 3 d (t_{-3}) before t_0. CO_2 was added from t_0 to t_6 every second day until target values were reached, and CO_2 addition was thereafter repeated 5 times over the course of the experiment to maintain high CO_2 levels. Measured pCO_2 and pH levels ranged from 272–370 µatm and 8.16–8.07, respectively, for the ambient pCO_2 treatment and from 1720–2250 µatm and 7.33–7.42, respectively, for the high pCO_2 treatment (Spisla et al. 2020).

2.2. Plankton sampling and counting

Plankton samples for light microscopy were taken every 4th day with a depth-integrated water sampler (Hydrobios) which was hauled from the mesocosms (maximum depth 20 m). For phyto- and protozooplankton counts, a volume of 250 ml was filled into brown glass bottles and acidic Lugol's iodine was added (to a final concentration of ~1%).

Phyto- and protozooplankton in the size range of 20–200 µm were counted after Utermöhl (Utermöhl 1958, Edler & Elbrächter 2010) at 100 and 200× magnification using inverted microscopes (ZEISS Axiovert 200 and Leica DM IRB/E) and 50/100 ml settling chambers. Microplankton taxa were identified to species or genus level using identification guides by Pankow (1990), Hoppenrath et al. (2009) and Kraberg et al. (2010). For ciliates, Kahl (1932) was used as well.

For biovolume estimates of the most abundant phyto- and protozooplankton species, geometric proxies of 10 individuals were measured according to Hillebrand et al. (1999). Thereafter, microalgae and dinoflagellate carbon content was calculated according to Menden-Deuer & Lessard (2000), while for ciliates, conversion factors given in Putt & Stoecker (1989) were used. For less abundant species, mean biovolumes according to Helsinki Commission data (Olenina et al. 2006) were used as proxies.

The 11 most abundant diatom and dinoflagellate species in terms of numbers and biomass were counted every 4th day in order to obtain high-temporal-resolution data on these specific species. Additionally, all identified *Ceratium* species were counted throughout the experiment (Table S1 in the Supplement at www.int-res.com/articles/suppl/m647p049_supp.pdf). An overview of trophic modes of the identified dinoflagellates is provided in Table S2. Ciliates were enumerated at intervals of 4 and 8 d. For species composition analysis, samples at t_3 and t_{49} were screened for all species, including rare taxa. To examine whether there was a treatment effect on size of the most predominant taxon *C. longipes* (the species contributing most to the overall biomass in all treatments), as well as for a less dominant congener (*C. fusus*) at t_2 and t_{47}, biovolume of these species was calculated.

Small phytoplankton were examined using flow cytometry. Samples for flow cytometry were taken each sampling day from gently mixed 10 l carboys immediately after the sampling boats returned. From each well-mixed sample, all particles were counted within 3 h with an Accuri C6 flow cytometer (BD Biosciences). Gates for phytoplankton cell detection were either based on particle forward scatter (FSC) and red chlorophyll fluorescence (FL3), FSC and orange fluorescence (FL2) signal (*Synechococcus*), FSC and far-red fluorescence (FL4) signal (cryptophytes) or side scatter (SSC) and FL3 (*Emiliania huxleyi*). Phytoplankton size classes were determined using the FSC signal (which correlates positively with particle size) and size-selective filtration of mesocosm samples with 0.2, 0.4, 0.6, 2.0, 3.0, 5.0, 8.0 and 10.0 µm polycarbonate filters. Based on FSC-related particle size and the additional fluorescence signal characteristics explained above, we assigned the detected phytoplankton cells into the following groups: picoeukaryotes (0.2–2.0 µm), small nano-eukaryotes (2.0–8.0 µm), large nano-eukaryotes (>8 µm), cryptophytes (3.0–10.0 µm), *E. huxleyi* (5.0–10.0 µm), FL4 cells (0.6–10.0 µm) and *Synechococcus*-like cells (0.6–3.0 µm). The abundance of larger phytoplankton cells (>20 µm) was assessed by light microscopy as outlined above. The abundance of phytoplankton cells per ml was calculated from the particles detected in each respective gate and the sub-sample volume measured. Approximate cell diameters were calculated as: estimated cell diameter = $0.0064 \times \mathrm{FSC}^{0.5262}$, using FSC values from Taucher et al. (2017), who reported a comprehensive evaluation of particle sizes and corresponding FSC signals with the same Accuri C6 flow cytometer used here.

2.3. FA analyses

Samples for FA analysis were filtered with Whatman GF/F filters (pore size: 0.7 µm). The filters were stored at −80°C in 2 ml Eppendorf tubes until further analysis. FA composition of filtered seston was determined by gas chromatography (GC). Lipids were extracted from the filters using a 1:1:1 solvent mix of dichloromethane:methanol:chloroform, cleaned up and esterified according to Arndt & Sommer (2014). As internal standards, C19.0 (as a fatty acid methy ester, FAME) and C21:0 (as a FA) were added to the samples (Restek), therefore allowing us to monitor esterification efficiency. In the first clean-up procedure, we used a 1 mol l^{-1} potassium chloride solution; the lower liquid phase was collected, and dried sodium sulfate was added to remove possible residual water. Samples were transferred to glass cocoons, and 200 µl 1% H_2SO_4 and 100 µl toluene were added for esterification, which took place overnight at 50°C. Thereafter, FAMEs were cleaned up with a 5% sodium chloride solution and n-hexane. The solvent phase was transferred to 100 µl n-hexane and a 1 µl aliquot measured in a Thermo Fisher Trace GC Ultra with a Thermo Fisher TRACETM TR-FAME column (10 m × 0.1 mm × 0.2 µm) using helium as carrier gas and a flame-ionization detector. The temperature program was 1 min at 50°C, heating 3 min to 150°C, 5 min to 155°C, 1.25 min to 165°C and 3.75 min to 240°C. To identify components, a 37 component FAME-mix (Supelco) and a Bacterial Acid Methyl Ester (BAME)-mix were used as references, and chromatograms were analyzed using the Chrom-Card Trace-Focus GC software. For further analysis, components were excluded where more than 50% of the values were zero, the maximal value was below 1% of total FAs or the mean value was below 0.5% of total FAs. Thus, from 49 components identified, 15 FAs remained.

2.4. Calculations and statistics

To assess treatment-dependent effects on plankton succession over time, a repeated measure ANOVA (RM-ANOVA) was performed using microplankton biomass and FA content data. For species composition data, Pielou's evenness (E) and the Shannon-Wiener Index (H') were calculated as follows:

$$H' = -\Sigma p_i \times \ln p_i \text{ with } p_i = \frac{n_i}{N} \quad (1)$$

where N is the total number of individuals and n_i is the number of individuals of 1 species, and

$$E = \frac{H'}{\log(S)} \quad (2)$$

where S is the number of species.

Both indices as well as the biovolume were compared between treatments (RM-ANOVA) after testing for normal distribution (Shapiro-Wilk test) and homogeneity of variances (Levene's test). If assumptions for parametric tests were not met, data were square-root transformed. Furthermore, non-metrical multidimensional scaling (NMDS) plots were generated (using Bray distance and 2 dimensions) and ANOSIMs (using the Bray-Curtis dissimilarity and 999 permutations) were conducted to depict the treatment effects on species composition (based on abundance data, in cells ml^{-1}) and FA composition (as ng l^{-1}). R v.3.2.2 (R Core Team 2017) was used for all analyses (packages 'lattice', 'nlme', 'vegan'; Sarkar 2008, Pinheiro et al. 2020, Oksanen 2011, respectively). All statistical tests were conducted at a significance level of $\alpha = 0.05$.

To explore the relationship between phytoplankton functional groups and the FAs determined in bulk seston samples, a principal component analysis (PCA) was performed on the mean values (biomass in µg C l^{-1} for phytoplankton; ng l^{-1} for FAs) of the 4 distinct experimental phases (see Section 3.1) for each mesocosm. Data were log transformed prior to analysis, and the R package 'ggfortify' (Tang & Horikoshi 2016) used for visualization.

3. RESULTS

3.1. Microplankton biomass development over time

Based upon the experimental procedures as well as the nutrient and chlorophyll *a* (chl *a*) dynamics (Spisla et al. 2020), the experimental period could be divided into 4 phases (vertical lines in Fig. 1). In brief, Phase I (t_{-3} to t_0) was the initial phase after closing the mesocosms and before the first CO_2 addition; in Phase II (t_1 to t_6) target pCO_2 values were reached (consequently, pH dropped from around 8.1 to 7.4) and chl *a* and nutrients decreased markedly; Phase III (t_7 to t_{26}) was a post-bloom phase where chl *a* values began to separate between treatments; and Phase IV (t_{27} to t_{49}) was a second post-bloom phase with enhanced treatment differences and a continued steady decline in chl *a*. Carbonate chemistry, particulate matter, nutrient and pigment concentration data are available at https://doi.pangaea.de/10.1594/PANGAEA.911638 (Spisla et al. 2020).

OA impacted total microplankton biomass. Phytoplankton in the microplankton size range (20–200 µm) was initially dominated by diatoms, with no apparent effect of increased pCO_2. Between t_{-3} and t_5 (Phases I and II) the community was dominated by different species of diatoms: *Guinardia delicatula*, *Dactyliosolen fragilissimum* and *Skeletonema marinoi.* There was no difference in diatom biomass between treatments (RM-ANOVA, $p = 0.7394$). Diatom biomass decreased from about 45 µg C l^{-1} at t_{-3} to values below detection limit at t_9 and did not reappear in detectable abundances in the mesocosms until the end of the experiment (Fig. 1a).

After the decline of the diatom biomass, dinoflagellates began to dominate (Phases III and IV). Nine days after the first CO_2 addition, significant differences between the treatments could be observed. While algal biomass increased steadily in the ambient pCO_2 treatment, it declined in the high pCO_2 treatment. The variances between mesocosms were much higher in the ambient treatments and much more conservative in the high pCO_2 treatments. Dinoflagellates contributed around 20 µg C l^{-1} initially. After t_5, communities in the high and ambient pCO_2 treatments diverged. In the high pCO_2 treatment, values decreased to around 10 µg C l^{-1} at the end of Phase III and remained low throughout Phase IV (mean ± SD: 12.5 ± 4.5 µg C l^{-1} at t_{49}). Biomass in the ambient pCO_2 treatment increased to 40.7 ± 8.69 µg C l^{-1} at t_{49} (Fig. 1b). Biomass was significantly higher in the ambient pCO_2 treatment than under increased pCO_2 levels (RM-ANOVA, $p < 0.001$) for the whole experiment. It must be noted that dinoflagellate communities comprised species with an auto-/mixotrophic feeding mode (e.g. *Ceratium* spp.) as well as purely heterotrophic species (e.g. *Gyrodinium fusiforme*, *Protoperidinium bipes*).

In both treatments, *Ceratium* was the dominant genus of microplankton throughout most of the experiment; *C. longipes* dominated while other species were present in lower numbers (Fig. 2). *Ceratium* spp. comprised 31.2 ± 6.0 and 23.5 ± 8.2% of microplankton cell numbers in the ambient and high pCO_2 treatments, respectively, and 46.7 ± 1.5 and 44.8 ± 1.8% of total microplankton biomass in the ambient and high pCO_2 treatment, respectively. For both treatments, *Ceratium* spp. were more evenly distributed in the beginning, but the community developed to a *C. longipes*-dominated system after about 10 (high pCO_2) and 20 (ambient pCO_2) experimental days. At the end of the experiment, *C. longipes* constituted almost 90% of the calculated *Ceratium* biomass in the ambient pCO_2 treatment,

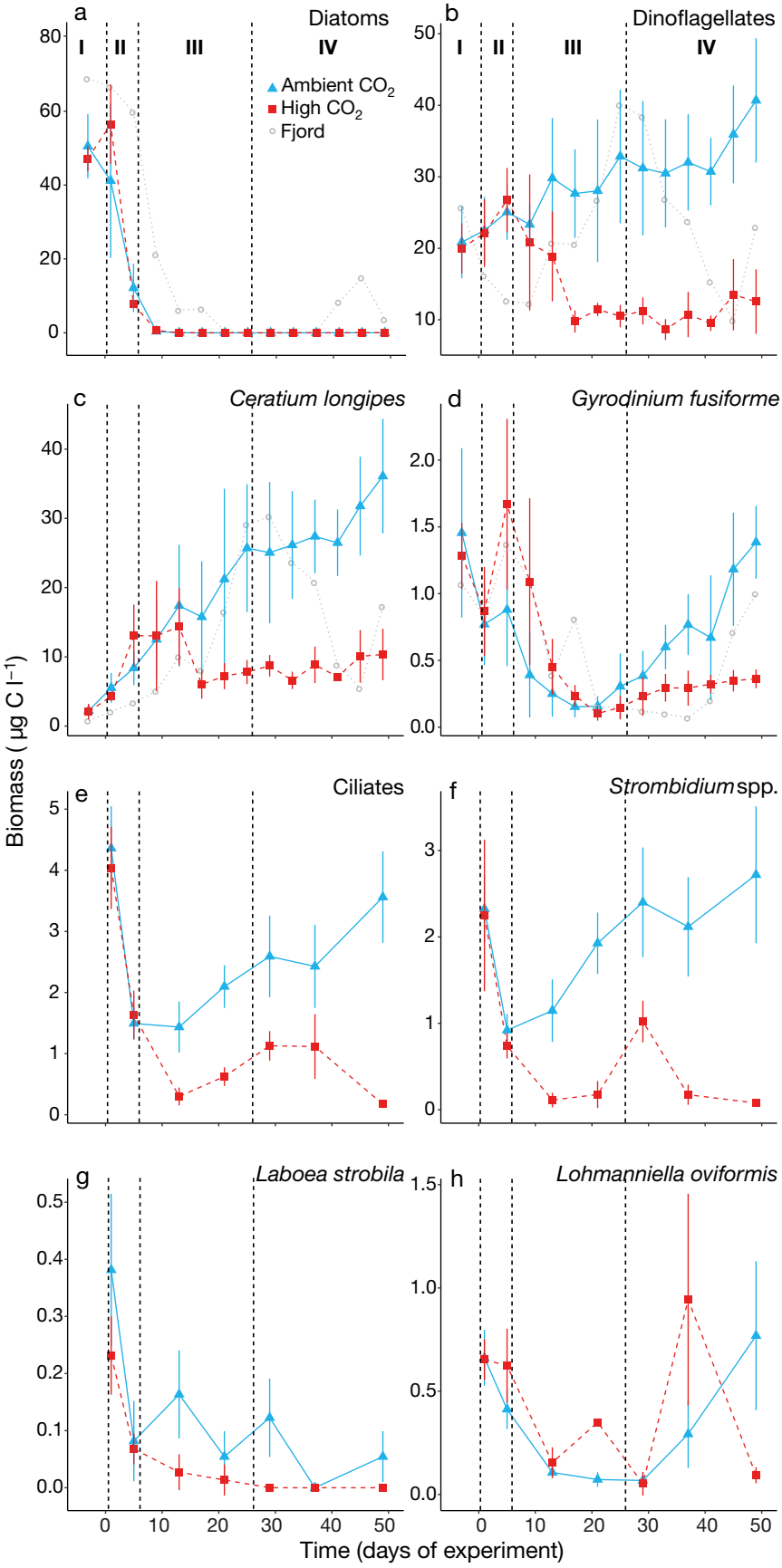

leaving the other 10% to the other 3 species, *C. fusus*, *C. tripos* and *C. macroceros* (Fig. 2a). For the high pCO_2 treatment (Fig. 2b), *C. longipes* made up only ~80% of calculated *Ceratium* biomass, leaving 20% for the remaining 3 species.

The biomass of *C. longipes* was significantly higher in the ambient pCO_2 treatment (RM-ANOVA, p = 0.0006), with mean values of 36.09 ± 8.28 and 10.33 ± 3.72 µg C l^{-1} at t_{49} for the ambient and high pCO_2 treatment, respectively (Fig. 1c).

The heterotroph dinoflagellate *G. fusiforme* contributed only lower shares to overall dinoflagellate biomass and increased significantly in the ambient pCO_2 treatment in the second half of the experiment (Fig. 1d). RM-ANOVA revealed a highly significant interaction between sampling days and treatment (p < 0.0001, Table 1).

Ciliates contributed less than 5 µg C l^{-1} to the microplankton community with a mean of 3.3 ± 1.4% in the ambient and 2.6 ± 1.9% contribution to total microplankton biomass, respectively. After an initial sharp decrease to <2 µg C l^{-1} in both treatments, ciliate biomass rebounded in the ambient pCO_2 treatment and remained significantly higher than in the high pCO_2 treatment (Fig. 1e). This was mainly due to the contribution of *Strombidium* spp. of different sizes (comprising *S.* cf. *capitatum*, *S.* cf. *depressum*, a very small unidentified species and, at the very end of the experiment, *S.* cf. *emergens*; see Table 1). While *Lohmanniella oviformis* was abundant (Fig. 1h) and contributed substantially

Fig. 1. Mean (±SD) biomass of (a) diatoms, (b) dinoflagellates, (c) *Ceratium longipes*, (d) *Gyrodinium fusiforme*, (e) ciliates, (f) *Strombidium* spp., (g) *Laboea strobila* and (h) *Lohmanniella oviformis* over the course of the experiment in the ambient (blue triangles) and high (red squares) pCO_2 treatment as well as in the fjord outside of the mesocosms (grey circles). Vertical dashed lines: the 4 major phases of the experiment

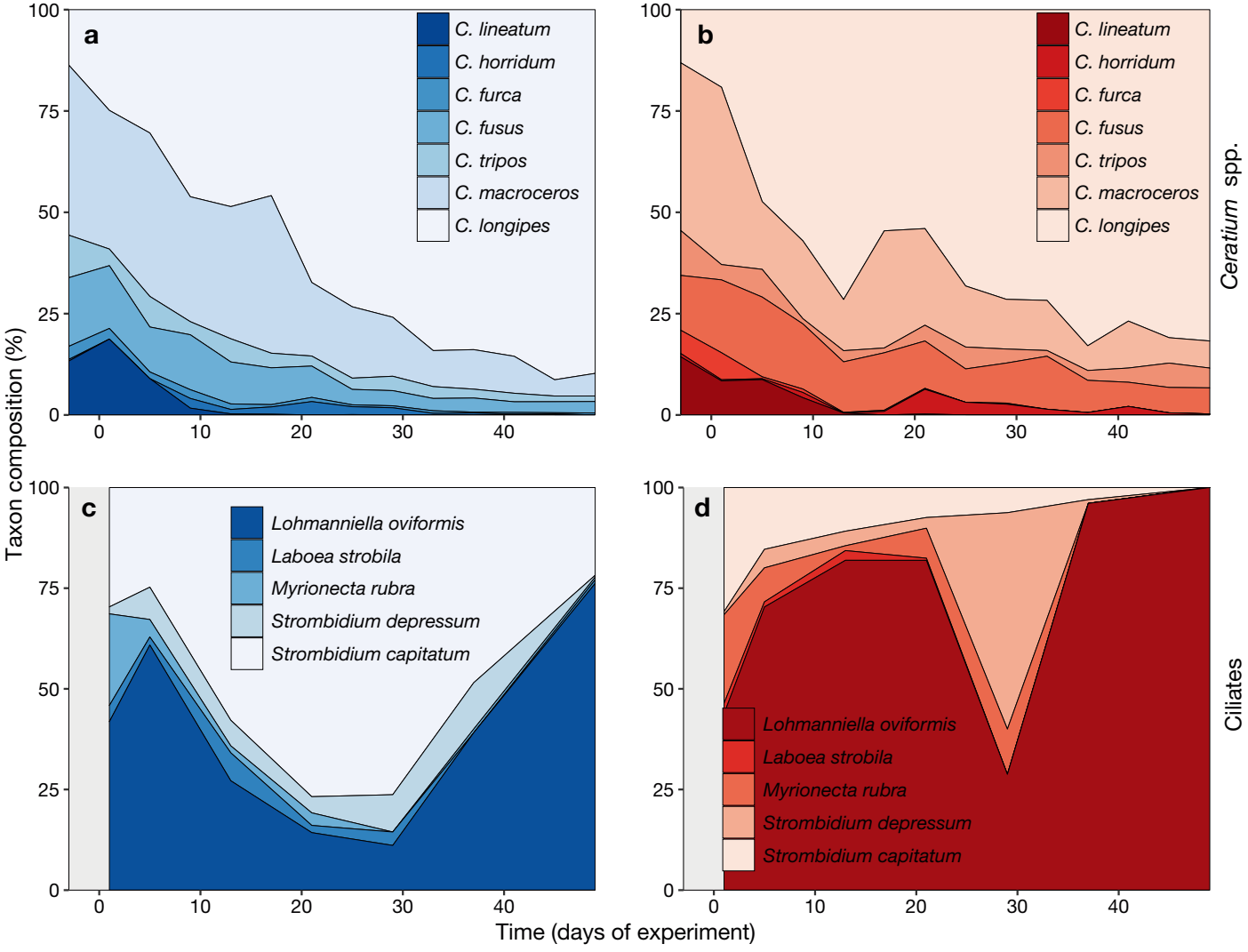

Fig. 2. Stacked graphs of taxon composition over time of the experiment for the predominant dinophyte genus *Ceratium* under (a) ambient and (b) high pCO_2 conditions, and for the predominant ciliate species *Strombidium* spp., *Myrionecta rubra*, *Lohmanniella oviformis* and *Laboea strobila* under (c) ambient and (d) high pCO_2 conditions

to ciliates (Fig. 2), it did not contribute substantially to total biomass due to its small size, and no significant treatment effect was observed. From those species that contributed less to total abundance and biomass — *Myrionecta rubra*, *Balanion comatum* and *Laboea strobila* — only *L. strobila* was significantly lower in the high pCO_2 treatment (Fig. 1g, Table 1).

3.2. Biovolume comparison of *C. longipes* and *C. fusus* (t_{-2} vs. t_{47})

Between t_{-2} and t_{47}, the biovolume of *C. longipes* decreased in the ambient pCO_2 treatment, with mean values of 11.5 ± 2.1 and 8.0 ± 0.9 $\times 10^4$ µm^3, respectively (Fig. 3a) (post hoc pairwise *t*-test, Bonferroni corrected, p = 0.034), but increased slightly in the high pCO_2 treatment (Fig. 3b) (t_{-2}: 11.1 ± 0.89 $\times$ 10^4 µm^3; t_{47}: 12.3 ± 1.1 $\times$ 10^4 µm^3; post hoc pairwise *t*-test, Bonferroni corrected, p = 0.073). The biovolume of *C. fusus* did not change significantly between days and treatments (Fig. 3b) (RM-ANOVA, days: df = 6, p = 0.0942; treatment: p = 0.2152).

3.3. Comparison of species and FA composition during experimental phases

For a list of all species identified during the course of the experiment, see Table S1. To investigate ef-

Table 1. Repeated measure ANOVA results for biomass development over time for the 19 most important species. Treatment: ambient pCO_2, high pCO_2; day: t_{-3} to t_{49}, except as indicated by superscripts: $^1t_{-3}$ to t_1; $^2t_{-3}$ to t_5; $^3t_{-3}$ to t_9. **Bold** indicates $p < 0.05$

Species	Treatment		Day		Treatment:day	
	F	p	*F*	p	*F*	p
Dactyliosolen fragilissimus[3,a]	1.4159	0.2790	121.16	**<0.0001**	0.1139	0.9508
Guinardia flaccida[3,a]	0.0058	0.9417	171.57	**<0.0001**	1.0582	0.3913
Guinardia delicatula[2,a]	0.1306	0.7302	11.2574	**0.0018**	3.8300	0.0517
Skeletonema marinoi[1,a]	0.0175	0.8992	146.95	**<0.0001**	0.6324	0.4568
Bacillariophyceae total[3,a]	0.1214	0.7394	184.66	**<0.0001**	3.0038	0.0576
Ceratium fusus[a]	0.6404	0.4541	18.3985	**<0.0001**	1.9014	**0.0425**
Ceratium longipes[a]	42.1191	**0.0006**	14.3973	**<0.0001**	7.0830	**<0.0001**
Ceratium macroceros[a]	16.8818	**0.0063**	9.2420	**<0.0001**	2.0819	**0.0245**
Ceratium tripos[a]	8.6248	**0.0261**	7.1730	**<0.0001**	2.6188	**0.0045**
Gymnodinium sp.[a]	0.4234	0.5393	34.7945	**<0.0001**	2.0239	**0.0293**
Gyrodinium fusiforme[a]	5.1008	**0.0647**	15.5338	**<0.0001**	5.3886	**<0.0001**
Protoperidinium depressum[a]	0.1243	0.7365	12.8594	**<0.0001**	1.0590	0.4065
Total dinophytes[a]	43.1893	**0.0006**	2.6721	**0.0038**	10.1540	**<0.0001**
Lohmanniella oviformis[a]	1.39	0.283	**24.44**	**<0.0001**	12.71	**<0.0001**
Laboea strobila[a]	32.11	**0.0013**	23.33	**<0.0001**	3.41	**0.0091**
Myrionecta rubra[a]	0.42	0.5414	73.13	**<0.0001**	2.47	**0.0420**
Strombidium capitatum[a]	119.65	**<0.0001**	30.88	**<0.0001**	20.46	**<0.0001**
Strombidium depressum[a]	5.66	0.0548	7.23	**<0.0001**	2.92	**0.0198**
Strombidium emergens	98.44	**<0.0001**	98.44	**<0.0001**	98.44	**<0.0001**
Small *Strombidium* sp.[a]	2.61	0.1572	68.37	**<0.0001**	50.21	**<0.0001**
Balanion comatum	8.99	**0.0240**	9.00	**<0.0001**	9.00	**<0.0001**
Total ciliates	65.75	**0.0002**	41.6	**<0.0001**	11.4	**<0.0001**

[a]Square-root transformed data

fects of high pCO_2 on the diversity of the plankton community, total species composition (including rare species and taxa) was compared between treatments at t_{-3} and t_{49} (Fig. 4). Overall species richness (number of species) was higher in the beginning than at the end of the experiment (Fig. 4a), with 52 ± 2.2 and 15 ± 2.6 species, respectively, and there was no significant difference between treatments at t_{49} (ambient: 15 ± 2.0, high: 14 ± 3.3; post hoc pairwise *t*-test, Bonferroni corrected, p = 0.78). *E* significantly increased over time, with mean score values of 0.49 ± 0.020 and 0.65 ± 0.079 at t_{-3} and t_{49}, respectively (Fig. 4b) (RM-ANOVA, df = 6, $p < 0.001$). This increase in *E* was larger in the high pCO_2 treatment. At t_{49}, *E* was significantly higher in the high pCO_2 treatment (post hoc pairwise *t*-test, Bonferroni corrected, $p < 0.05$), with a mean value of 0.71 ± 0.04 and 0.60 ± 0.07 in the high and ambient treatment, respectively (Fig. 4b). In contrast to *E*, *H′* decreased over time (Fig. 4c) (RM-ANOVA, df = 6, $p < 0.05$), which was mainly due to the pronounced decrease in the ambient pCO_2 treatment: at t_{49}, *H′* behaved similarly to *E*. *H′* was higher in the high pCO_2 treatment (post hoc pairwise *t*-test, Bonferroni corrected, $p < 0.01$), with mean values of 1.87 ± 0.13 and 1.61 ± 0.12 in the high and ambient treatment, respectively (Fig. 4c). Both species and FA composition changed significantly over time (Fig. 5) (ANOSIM, $p < 0.05$). Within phases of the experiment, the plankton communities were similar between treatments in Phase II (Fig. 5a) (ANOSIM, p = 0.655), but significantly different in Phase IV (Fig. 5a) (ANOSIM, $p < 0.05$). Likewise, FA composition was similar between treatments during Phase I (ANOSIM, p = 0.15), but significantly different between high and ambient pCO_2 treatments during Phase IV (Fig. 5b) (ANOSIM, $p < 0.05$).

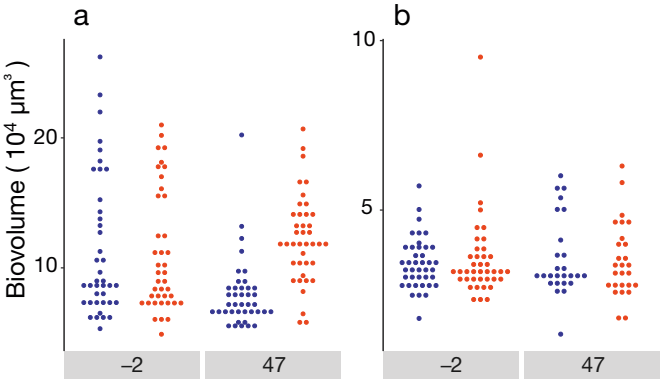

Fig. 3. Biovolume distributions of (a) *Ceratium longipes* and (b) *C. fusus* 2 d before (t_{-2}) and 47 d after (t_{47}) the start of experimental manipulation for ambient (blue) and high (red) pCO_2 conditions

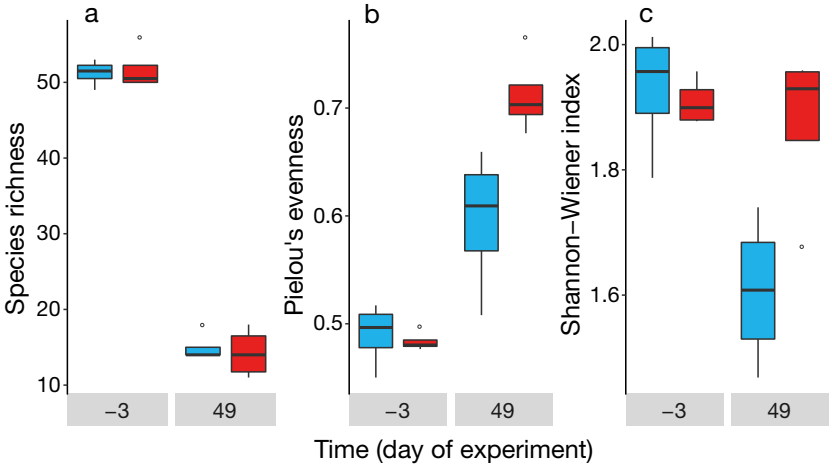

Fig. 4. (a) Species richness, (b) Pielou's evenness and (c) Shannon-Wiener index under ambient (blue) and high (red) pCO_2 conditions 3 d before (t_{-3}) and 49 d after (t_{49}) the start of experimental manipulation. Horizontal lines: medians; boxes: 25th to 75th percentile range; whiskers: 1.5 × interquartile range; dots: outliers

3.4. FA content development over time

The total FA content of seston continuously decreased over the course of the experiment in both treatments (and was lower than the field samples), but with significantly higher values in the ambient pCO_2 treatment, particularly towards the end of the experiment (Fig. 6a) (RM-ANOVA, $p < 0.01$). Carbon-specific total FA content of seston (calculated with particulate organic carbon content per liter from parallel samples, available from Spisla et al. 2020) ranged between approximately 1 and 2.5 ng FA μg^{-1} C, with no significant differences between treatments or over time. However, the ratios of both monounsaturated fatty acids (MUFAs) and PUFAs to saturated fatty acids (SFAs) were significantly higher in the ambient pCO_2 treatment (Fig. 6b,c) (RM-ANOVA, $p < 0.05$ and $p < 0.01$, respectively). Over the course of the experiment, a treatment effect on several specific FAs was detected (Table 2). For example, FAs that were significantly lower in the high pCO_2 treatment included the PUFAs DHA and EPA as well as C14:0 (Fig. 6d–f, Table 2). In general, the temporal development in FA composition reflected the succession from a diatom-dominated plankton bloom to a dinoflagellate-dominated post-bloom community. Concentrations of diatom marker FAs (EPA, C16:1*n*7) were highest in the beginning. After their sharp decrease, total FAs were dominated by dinoflagellate marker FAs (DHA, C14:0).

3.5. Relationship between planktonic groups and FAs

The first 2 principal components of the PCA explained 65.9% of the variance in the data. The biplot along the axes of PC1 and PC2 revealed that the data clustered together during Phases I and II, but separated between treatments in Phases III and IV (Fig. 7). Initially, ciliate biomass was relatively high, with a subsequent decline during Phase II. In Phase III, the relative importance of nano- and picophytoplankton increased (the latter being signifi-

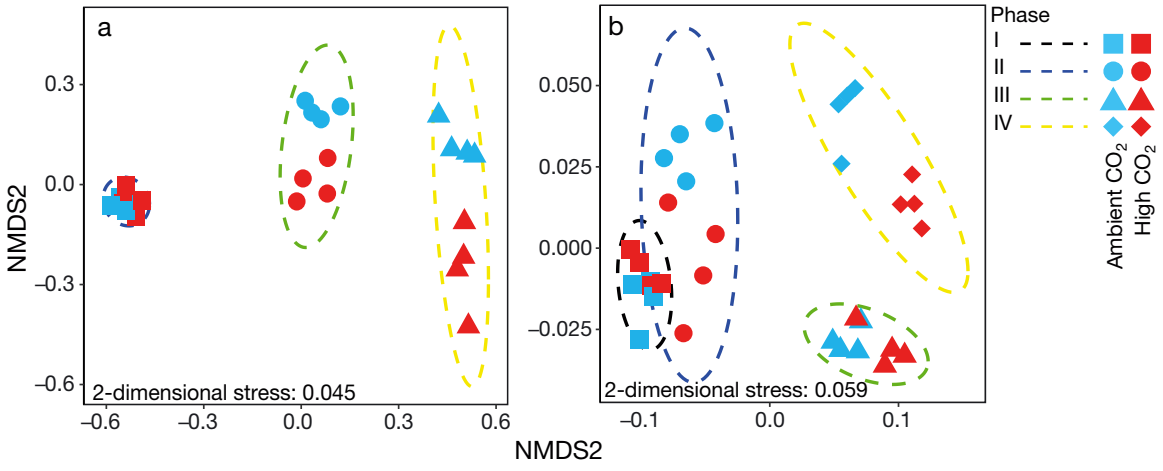

Fig. 5. Non-metrical multidimensional scaling of the (a) plankton community composition and (b) fatty acid composition during the experiment. Values are mesocosm mean values of the 4 experimental phases (see Fig. 1); 95% confidence ellipses for the respective phases are indicated

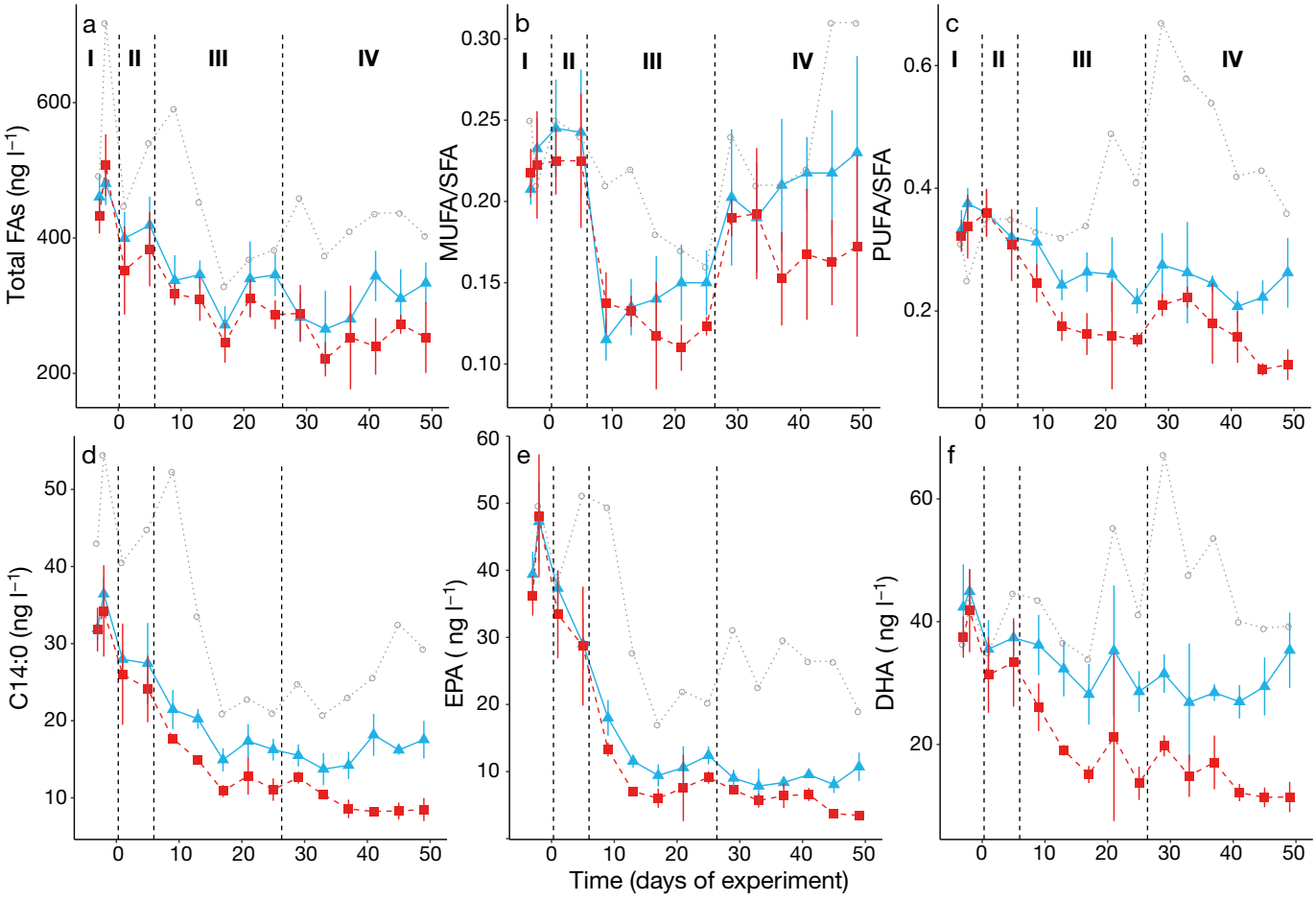

Fig. 6. Mean (±SD) (a) total fatty acids (FAs), (b) monounsaturated fatty acid (MUFA) to saturated fatty acid (SFA) ratio, (c) polyunsaturated fatty acid (PUFA) to SFA ratio, (d) C14:0, (e) eicosapentaenoic acid (EPA) and (f) docosahexaenoic acid (DHA) content over the course of the experiment in the ambient (blue triangles) and high (red squares) pCO_2 treatments as well as in the fjord outside of the mesocosms (grey circles). Vertical dashed lines: the 4 major phases of the experiment

cantly higher in the high pCO_2 treatment) and finally, increasing contributions of *Synechococcus* (in particular in the ambient pCO_2 treatment) and cryptophyceans (with no treatment difference) occurred in the plankton community in Phase IV. The spread occurred along both axes in a way that values from the high pCO_2 treatment scored higher along PC1 and lower along PC2 than those from the ambient pCO_2 treatment. Total ciliates and dinoflagellates were positively correlated with each other and with the FAs 16:1*n*7, DHA, 18:1*n*9 and 18:1*n*7. They were negatively correlated with pico- and nanophytoplankton (from flow cytometry) and the FA 22:1*n*9. Total diatoms and *Emiliania huxleyi* were positively correlated with each other and the FAs EPA, 16:0, 17:0, 18:4*n*3 and 3-OH-14:0. No FA was highly positively correlated with the *Synechococcus* or the Cryptophyceae group.

4. DISCUSSION

4.1. Biomass development over time

We used a mesocosm approach to investigate the effects of extreme OA on a coastal post-bloom plankton community dominated by dinoflagellates. In both high and ambient pCO_2 conditions, the dominant dinoflagellates and ciliates were strongly negatively affected. In general, the interpretation of any results obtained from mesocosm experiments should consider possible enclosure effects. With increasing experimental duration, the community composition and succession in mesocosms may deviate from that in the natural environment, particularly in small enclosures (e.g. Hauss et al. 2012). Logistical effort restricts the number of mesocosms and treatment levels (e.g. in our case, intermediate pCO_2 values).

Table 2. Repeated measure ANOVA results for fatty acid (FA) content development (in ng l^{-1}) over time. EPA: eicosapentaenoic acid; DHA: docosahexaenoic acid; SFA: saturated fatty acid; MUFA: monounsaturated fatty acid; PUFA: polyunsaturated fatty acid. Treatment: ambient pCO_2, high pCO_2; day: t_{-3} to t_{49}. **Bold** indicates p < 0.05

	Treatment		Day		Treatment:day	
	F	p	*F*	p	*F*	p
C 14:0[a]	51.4410	**0.0004**	91.7060	**<0.0001**	5.0150	**<0.0001**
C 15:0	0.9526	0.3667	14.2019	**<0.0001**	0.8260	0.6393
C 16:0	5.2890	0.0611	22.9760	**<0.0001**	0.9050	0.5563
C 16:1n7[a]	52.4060	**0.0004**	94.7860	**<0.0001**	6.2990	**<0.0001**
C 17:0[a]	4.6510	0.0744	187.2240	**<0.0001**	1.0060	0.4554
C 18:0[a]	0.2440	0.6388	1.6000	0.0964	0.8060	0.6600
C 18:1n9c	2.4911	0.1656	5.0883	**<0.0001**	1.8183	**0.0494**
C 18:1n7	39.8958	**0.0007**	7.9115	**<0.0001**	6.9293	**<0.0001**
C 18:2n6c[a]	21.0970	**0.0037**	10.7850	**<0.0001**	1.4360	0.1554
C 3-OH-14:0[a]	0.0225	0.8857	15.5278	**<0.0001**	0.7651	0.7028
C 18:3n3[a]	20.8330	**0.0038**	10.3610	**<0.0001**	5.3850	**<0.0001**
C 18:4n3[a]	7.4810	**0.0340**	20.5930	**<0.0001**	2.7530	**0.0022**
C 20:5n3c[a] (EPA)	19.1810	**0.0047**	159.2330	**<0.0001**	2.0610	**0.0226**
C 22:1n9c	0.2444	0.6386	19.5721	**<0.0001**	0.8155	0.6504
C 22:6n3c (DHA)	38.6754	**0.0008**	18.0183	**<0.0001**	2.6241	**0.0034**
Total FA	16.3400	**0.0068**	25.4730	**<0.0001**	1.2150	0.2809
SFA	3.9490	0.0941	12.0930	**<0.0001**	0.8650	0.5986
MUFA	12.4861	**0.0123**	25.4829	**<0.0001**	2.0734	**0.0217**
PUFA	27.1501	**0.0020**	51.8758	**<0.0001**	1.6522	0.0825
16:1/16:0	34.1720	**0.0011**	53.8924	**<0.0001**	6.4895	**<0.0001**
MUFA:SFA	10.7530	**0.0168**	14.4530	**<0.0001**	1.6320	0.0877
PUFA:SFA	19.1640	**0.0047**	22.4365	**<0.0001**	2.3260	**0.0094**

[a]Square-root transformed data

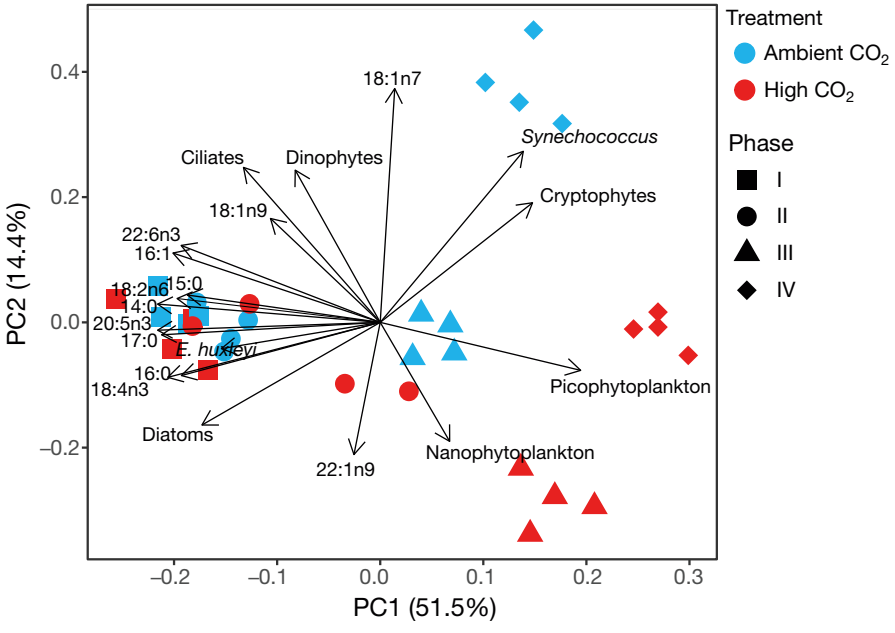

Fig. 7. Principal component analysis exploring the relationship between major planktonic groups (based upon microscopic counts and flow cytometry) and fatty acids measured in bulk seston under high and ambient pCO_2 experimental treatments

Observed responses to natural communities should be extrapolated with caution and should account for a possible mesocosm bias. In addition, the initial enclosed community as well as environmental conditions other than the manipulated factor need to be considered. All observed effects may only impact those species that are tolerant to mesocosm conditions, and important components of natural communities may have been lost in the mesocosm setup.

Despite these constraints and their variable nature, mesocosm experiments can help us understand effects beyond single-organism responses. The succession from a diatom-dominated to a dinoflagellate-dominated community observed in our experiment is a common pattern during spring–summer transition in temperate oceans (Smetacek & Hendrikson 1979, Smetacek 1981). From a clearly diatom-dominated community in Phase I, the experimental plankton community quickly moved to a dinoflagellate-dominated community in Phase II. Shortly after the initial experimental phases the system experienced nutrient depletion, thus making it impossible to observe treatment effects on diatoms. The chl *a* concentrations (Spisla et al. 2020) closely depicted the development of the diatom community, but did not fit the development of the dinoflagellate biomass, indicating the importance of mixotrophy/heterotrophy in explaining the overall plankton biomass development in this study. Mixotrophic dinoflagellates, including species of the genus *Ceratium*, have a high carbon/chl *a* ratio (Geider 1987, Lyngsgaard et al. 2014) and contribute more to particulate organic carbon than to chl *a*. Interestingly, the variances between mesocosms were much higher in the ambient treatments and much more conservative in the high pCO_2 treatments, indicating that acidification had a strong streamlining effect on phytoplankton biomass responses.

Increases in pico- and nanophytoplankton fractions are commonly known to stimulate growth and reproduction of micrograzers such as ciliates and heterotrophic dinoflagellates (Löder et al. 2011, Aberle et al. 2013). Similar patterns were observed in the present study at ambient pCO_2, with clear increase in ciliates and heterotrophic dinoflagellates with increasing pico- and nanophytoplankton biomass pointing at distinct predator–prey relationships between these groups.

Elevated pCO_2 is usually thought to stimulate autotroph production due to a higher availability of CO_2 for photosynthesis. Thus, increases in autotroph production are an expected phenomenon under elevated pCO_2 and may lead to a higher abundance of the primary producer if the effect is not mitigated by grazing. A positive effect of elevated pCO_2 on abundances of autotrophic dinoflagellates was reported in Horn et al. (2016). Negative impacts of OA on autotrophic dinoflagellates are a rarely described response so far (see e.g. Leu et al. 2013, Eberlein et al. 2014, Hennon et al. 2017). In a recent study, the negative effects of high pCO_2 on dinoflagellates were considered to be linked to low nutrient availability (Alvarez-Fernandez et al. 2018). Autotrophic dinoflagellates are known for their effective CCMs that prevent CO_2 limitation. Excess CO_2 can lead to a down-regulation of CCMs, thus reducing the costs of acquiring inorganic carbon and making energy available for other purposes, e.g. nutrient acquisition (Rost et al. 2006, Eberlein et al. 2016). Such a down-regulation in CCMs can be an effective strategy, especially during periods of nutrient limitation. While down-regulation of CCMs seems to be beneficial for phytoplankton in energetic terms, it can in turn lead to physiological constraints during photosynthesis, e.g. reduced nutrient assimilation with potential negative effects on phytoplankton standing stocks (Eberlein et al. 2016). Accounting for CCM regulation mechanisms and plankton community-specific responses under a post-bloom scenario (Sala et al. 2016) might thus explain the negative responses of autotrophic dinoflagellates (in this case, particularly *C. longipes*) under elevated pCO_2 conditions. *C. longipes* can be kept in autotrophic monoculture (Boulding & Platt 1986) and has been observed as a largely photosynthetic species in the field (Taguchi 1981). Therefore, this species was considered mainly as an autotroph in this study. However, phagocytosis in *C. longipes* has also been reported (Jacobson & Anderson 1996).

Similar to autotrophic dinoflagellates, the abundance and biomass of micrograzers such as ciliates and heterotrophic dinoflagellates was reduced under OA compared to ambient conditions. While several previous studies pointed at the insensitivities of ciliates and heterotrophic dinoflagellates to elevated pCO_2 (Suffrian et al. 2008, Aberle et al. 2013), some have also shown negative effects on specific species or groups of heterotrophic dinoflagellates (Hinga 2002, Pedersen & Hansen 2003). In the present study, reduced total ciliate biomasses were found in *Strombidium* spp. and *Laboea strobila* at elevated pCO_2 conditions, while biomass of *L. oviformis* remained unaffected. The biomass of the heterotrophic dinoflagellate *Gyrodinium fusiforme* was reduced under OA only during the final phase of the experiment (Phase IV). Our data confirm the outcome of other mesocosm studies that report negative OA impacts on heterotrophic protists in natural plankton communities (Calbet et al. 2014, Horn et al. 2016). Negative effects on abundance, biomass or community composition of micrograzers under elevated pCO_2 conditions are commonly considered as indirect effects (e.g. via trophic cascades, competition, mutualism or interaction modifications) rather than direct OA impacts due to e.g. changes in physiology (Alvarez-Fernandez et al. 2018). One possible indirect pathway could be increased competitive ability by autotrophic species, for which higher pCO_2 levels may have fertilizing effects. Establishing a causality of indirect effects, however, would require experimental assessment.

It needs to be emphasized that the chosen high pCO_2 treatment simulated extreme CO_2 conditions. Impacts of intermediate pCO_2 within the open ocean prediction range on this plankton community would undoubtedly have been smaller, although it is unclear whether effects are linear. Also, comparatively rapid adaptation in single-cell microalgae (Lohbeck et al. 2012) may lead to weakened effects of continuously increasing oceanic pCO_2. Apart from these continuous effects, coastal systems are likely to encounter more frequent, intense and prolonged extreme events such as heat waves (Rahmstorf & Coumou 2011), including hypoxia/hypercapnia (Melzner et al. 2013).

4.2. Microplankton species composition and diversity

Both species richness and H' were high in the beginning, caused by the presence of a number of diatom species when nutrients were still readily available (>1 µmol l^{-1} NO_x). When the mesocosms were closed, NO_3 and NO_2 concentrations were

<0.5 µmol l^{-1} and further declined over the next few days to <0.2 µmol l^{-1} (Spisla et al. 2020). During the nitrogen-depleted post-bloom phase, the number of species declined, a pattern that is typical of a post-bloom succession (e.g. Sala et al. 2016).

As species were not evenly distributed (dominance of a single species), *E* was low in both treatments. The high *H'* in elevated pCO_2 conditions at t_{49} contrasts with a previous mesocosm study where plankton diversity remained unaffected by OA (Horn et al. 2016). However, in that study the focus was only on heterotrophic protists rather than the whole microplankton community. The higher *E* observed at elevated pCO_2 in the present study was mainly caused by lower abundance of the dominant species (e.g. *C. longipes*, *Strombidium capitatum*) in the high pCO_2 treatment.

4.3. Biovolume comparison for the dominant phytoplankton, *Ceratium*

The observed biovolume increase in *C. longipes* is in accordance with the expectation that increased CO_2 leads to an increase in cell size (Sommer et al. 2015) and the production rates of some autotrophic dinoflagellates (Eberlein et al. 2014). It has been hypothesized that either a release from CO_2-limitation or an increase in non-protein storage components would lead to larger cell sizes at increased pCO_2 (Sommer et al. 2015). At a comparable species-specific carbon concentrating capacity, larger-sized cells, in particular, are more competitive at high nutrient concentrations when uptake is not limited by diffusion, while smaller cells become efficient at low nutrient availability due to their high surface area to volume ratio (Finkel et al. 2010 and references therein). Thus, larger cells can be expected to show stronger responses to increased carbon availability under replete nutrient concentrations.

4.4. FA contents and composition

The development of several FA components over time mirrored the microplankton biomass patterns, indicating a predominant role of this size fraction in determining FA availability to higher trophic levels in this experiment. EPA and C14:0 content followed the diatom biomass, with a steep decline during Phase II (Fig. 6b,c); both FAs are associated with diatoms and *Emiliania huxleyi* (Dalsgaard et al. 2003). In Phases III and IV, the highest contribution to PUFAs was by DHA, which is a dinoflagellate marker FA (Dalsgaard et al. 2003 and references therein) and was significantly lower at increased CO_2. Accordingly, the pCO_2 treatment effects — which became apparent from Phase II on and increased over Phases III and IV — are predominantly explained along the dinoflagellate eigenvector. The largest treatment effect of CO_2 addition in Phases III and IV was in the opposite direction of the ciliate and dinoflagellate biomass as well as the FAs 18:1*n*7, 18:1*n*9, DHA and 16:1*n*7. The PCA results indicated that the main driver of FA composition change was the community structure shift, as was the case for an Arctic community during a mesocosm study in Kongsfjorden (Leu et al. 2013). It may still be possible that pCO_2 also influenced the cellular FA content as was, for example, shown for *Gymnodinium* spp. and *Pyramimonas gelidicola* (Wynn-Edwards et al. 2014).

PUFAs such as EPA and DHA are essential FAs for higher trophic levels. The latter are not able to produce essential FAs de novo, because they lack an enzyme important for introducing double bonds (Brett & Müller-Navarra 1997, Bell et al. 2007). Both DHA (provided by dinoflagellates) and EPA (provided by diatoms) are of particular importance for egg production in crustaceans (Müller-Navarra et al. 2000, Rossoll et al. 2012). A decrease in the ratio of PUFAs to SFAs in a phytoplankton species due to OA was found to negatively influence the growth and egg production of a copepod (Rossoll et al. 2012). High food quality (high concentration of essential FAs such as EPA and DHA in copepods) can be related to high growth rates of larval herring, and FAs produced by phytoplankton have been reported to transfer to *Clupea harengus* larvae via zooplankton (Fraser et al. 1989). Thus, the approximately 16% pCO_2-related difference we saw in TFA content at the protist level may entail consequences for higher trophic levels, including commercially important fish species. In particular, the essential FA DHA decreased by 51% in the final phase of our study, which was related to a 67% lower biomass of the key group of dinoflagellates. Although *Ceratium* spp. are not traditionally considered high quality prey for consumers, they are readily consumed by a variety of protozoans (e.g. Skovgaard 1996) and metazoans (e.g. Nielsen 1991).

5. CONCLUSIONS

The aim of this mesocosm campaign was to investigate pelagic community responses to OA. This study

showed the impact of OA on phyto- and protozooplankton abundance, diversity, community composition and nutritional quality, providing a basis for assessment of biomass and essential nutrient flux to higher trophic levels.

The experimentally altered pCO_2-increase caused exposure of higher trophic levels to a decreased microplankton biomass and lower food quality of this crucial plankton size fraction for mesozooplankton, entailing potential consequences for energy transfer efficiencies. Both in terms of quality and quantity of their food, higher trophic levels may thus experience worse conditions at the protist level, at the base of the food web, when exposed to increased pCO_2 levels, with potential cascading consequences for consumers. Future investigations should experimentally assess direct responses of *Ceratium* spp. to OA and other environmental factors, which may help to unravel under which conditions the dominance of dinoflagellates is altered. Further, more experimental multiple-stressor studies will be needed to assess plankton community responses (including effects on community functions of nutrient uptake and respiration) to interactions of major global climate-change related factors, i.e. OA, warming and deoxygenation.

Acknowledgements. We gratefully acknowledge funding for the KOSMOS 2015 campaign by the Kiel Excellence Cluster 'The Future Ocean' (CP1540), the Leibniz Award 2012 to U.R., a Norwegian-German Willy-Brandt MSc stipend awarded to I.D. (10-2015-S), and the SFB754 for supporting H.H. We thank Thomas Hansen for technical guidance in FAME analyses, the Bergen 2015 KOSMOS team, particularly Dana Michaelis, Anna Lechtenbörger and Henrike Wunderow for ecological discussion, Andrea Ludwig and Mathias Haunost for organizing logistics, the KOSMOS diving team for technical support and Annegret Stuhr for advice during plankton enumeration. Data used in the present study are publicly available at https://doi.pangaea.de/10.1594/PANGAEA.896337.

LITERATURE CITED

Aberle N, Schulz KG, Stuhr A, Malzahn A, Ludwig A, Riebesell U (2013) High tolerance of microzooplankton to ocean acidification in an Arctic coastal plankton community. Biogeosciences 10:1471–1481

Alvarez-Fernandez S, Bach LT, Taucher J, Riebesell U and others (2018) Plankton responses to ocean acidification: the role of nutrient limitation. Prog Oceanogr 165:11–18

Andersson M, Van Nieuwerburgh L, Snoeijs P (2003) Pigment transfer from phytoplankton to zooplankton with emphasis on astaxanthin production in the Baltic Sea food web. Mar Ecol Prog Ser 254:213–224

Arendt KE, Jónasdóttir SH, Hansen PJ, Gärtner S (2005) Effects of dietary fatty acids on the reproductive success of the calanoid copepod *Temora longicornis.* Mar Biol 146:513–530

Arndt C, Sommer U (2014) Effect of algal species and concentration on development and fatty acid composition of two harpacticoid copepods, *Tisbe* sp. and *Tachidius discipes*, and a discussion about their suitability for marine fish larvae. Aquacult Nutr 20:44–59

Bell MV, Dick JR, Anderson TR, Pond DW (2007) Application of liposome and stable isotope tracer techniques to study polyunsaturated fatty acid biosynthesis in marine zooplankton. J Plankton Res 29:417–422

Bermúdez JR, Riebesell U, Larsen A, Winder M (2016) Ocean acidification reduces transfer of essential biomolecules in a natural plankton community. Sci Rep 6: 27749

Bermúdez R, Feng YY, Roleda MY, Tatters AO and others (2015) Long-term conditioning to elevated pCO_2 and warming influences the fatty and amino acid composition of the diatom *Cylindrotheca fusiformis.* PLOS ONE 10:e0123945

Bermúdez R, Winder M, Stuhr A, Almén AK, Engström-Öst J, Riebesell U (2016) Effect of ocean acidification on the structure and fatty acid composition of a natural plankton community in the Baltic Sea. Biogeosciences 13:6625–6635

Bi R, Ismar SMH, Sommer U, Zhao M (2017) Environmental dependence of the correlations between stoichiometric and fatty acid-based indicators of phytoplankton food quality. Limnol Oceanogr 62:334–347

Bi R, Ismar SMH, Sommer U, Zhao M (2018) Simultaneous shifts in stoichiometric and fatty acid composition of *Emiliania huxleyi* in response to environmental changes. Biogeosciences 15:1029–1045

Boulding EG, Platt T (1986) Variation in photosynthetic rates among individual cells of a marine dinoflagellate. Mar Ecol Prog Ser 29:199–203

Brett MT, Müller-Navarra DC (1997) The role of highly unsaturated fatty acids in aquatic foodweb processes. Freshw Biol 38:483–499

Calbet A (2008) The trophic roles of microzooplankton in marine systems. ICES J Mar Sci 65:325–331

Calbet A, Sazhin AF, Nejstgaard JC, Berger SA and others (2014) Future climate scenarios for a coastal productive planktonic food web resulting in microplankton phenology changes and decreased trophic transfer efficiency. PLOS ONE 9:e94388

Dalsgaard J, St. John M, Kattner G, Muller-Navarra D, Hagen W (2003) Fatty acids as trophic markers in the pelagic marine environment. Adv Mar Biol 46:225–340

Eberlein T, Van de Waal D, Rost B (2014) Differential effects of ocean acidification on carbon acquisition in two bloom-forming dinoflagellate species. Physiol Plant 151: 468–479

Eberlein T, Van de Waal DB, Brandenburg KM, John U, Voss M, Achterberg EP, Rost B (2016) Interactive effects of ocean acidification and nitrogen limitation on two bloom-forming dinoflagellate species. Mar Ecol Prog Ser 543:127–140

Eberlein T, Wohlrab S, Rost B, John U, Bach LT, Riebesell U, Van de Waal DB (2017) Effects of ocean acidification on primary production in a coastal North Sea phytoplankton community. PLOS ONE 12:e0172594

Edler L, Elbrächter M (2010) The Utermöhl method for quantitative phytoplankton analysis. In: Karlson B, Cusack C, Bresnan E (eds) Microscopic and molecular methods for quantitative phytoplankton analysis. Manuals and Guides No. 55. UNESCO, Paris, p 13–20

Fabry VJ, Seibel BA, Feely RA, Orr JC (2008) Impacts of ocean acidification on marine fauna and ecosystem processes. ICES J Mar Sci 65:414–432

Field C, Behrenfeld M, Randerson J, Falkowski P (1998) Primary production of the biosphere: integrating terrestrial and oceanic components. Science 281:237–240

Finkel ZV, Beardall J, Flynn KJ, Quigga A, Rees TA, Raven JA (2010) Phytoplankton in a changing world: cell size and elemental stoichiometry. J Plankton Res 32:119–137

Fraser AJ, Sargent JR, Gamble JC, Seaton DD (1989) Formation and transfer of fatty acids in an enclosed marine food chain comprising phytoplankton, zooplankton and herring (*Clupea harengus* L.) larvae. Mar Chem 27:1–18

Geider RJ (1987) Light and temperature dependence of the carbon to chlorophyll *a* ratio in microalgae and cyanobacteria: implications for physiology and growth of phytoplankton. New Phytol 106:1–34

Gifford DJ (1991) The protozoan–metazoan link in pelagic ecosystems. J Protozool 38:81–86

Giordano M, Beardall J, Raven JA (2005) CO_2 concentrating mechanisms in algae: mechanisms, environmental modulation, and evolution. Annu Rev Plant Biol 56:99–131

Grossart H, Allgaier M, Passow U, Riebesell U (2006) Testing the effect of CO_2 concentration on the dynamics of marine heterotrophic bacterioplankton. Limnol Oceanogr 51:1–11

Harvey CJ, Williams GD, Levin PS (2012) Food web structure and trophic control in central Puget Sound. Estuar Coasts 35:821–838

Hauss H, Franz JMS, Sommer U (2012) Changes in N:P stoichiometry influence taxonomic composition and nutritional quality of phytoplankton in the Peruvian upwelling. J Sea Res 73:74–85

Hennon GMM, Hernández Limón MD, Haley ST, Juhl AR, Dyhrman ST (2017) Diverse CO_2-induced responses in physiology and gene expression among eukaryotic phytoplankton. Front Microbiol 8:2547

Hillebrand H, Dürselen CD, Kirschtel D, Pollingher U, Zohary T (1999) Biovolume calculation for pelagic and benthic microalgae. J Phycol 35:403–424

Hinga KR (2002) Effects of pH on coastal marine phytoplankton. Mar Ecol Prog Ser 238:281–300

Hoppenrath M, Elbrächter M, Drebes G (2009) Marine phytoplankton: selected microphytoplankton species from the North Sea around Helgoland and Sylt. Schweizerbart Science Publishers, Stuttgart

Horn HG, Sander N, Stuhr A, Alguero-Muniz M and others (2016) Low CO_2 sensitivity of microzooplankton communities in the Gullmar Fjord, Skagerrak: evidence from a long-term mesocosm study. PLOS ONE 11:e0165800

IPCC (2017) IPCC fifth assessment report (AR5) observed climate change impacts database, v2.01 (2007–2014). NASA Socioeconomic Data and Applications Center (SEDAC), Palisades, NY.

Jacobson DM, Anderson DM (1996) Widespread phagocytosis of ciliates and other protists by marine mixotrophic and heterotrophic thecate dinoflagellates. J Phycol 32: 279–285

Kahl A (1932) Urtiere oder Protozoa I. Wimpertiere oder Ciliata (Infusoria). In: Dahl F (ed) Tierwelt Deutschlands und der angrenzenden Meeresteile, Vol 18. Fischer, Jena, p 1–886

Kim JM, Lee K, Shin K, Kang JH and others (2006) The effect of seawater CO_2 concentration on growth of a natural phytoplankton assemblage in a controlled mesocosm experiment. Limnol Oceanogr 51:1629–1636

Klein Breteler WCM, Schogt N, Baas M, Schouten S, Kraay GW (1999) Trophic upgrading of food quality by protozoans enhancing copepod growth: role of essential lipids. Mar Biol 135:191–198

Kraberg A, Baumann M, Dürselen CD (2010) Coastal phytoplankton: photo guide for northern European seas. Pfeil, München

Le Quéré C, Andrew RM, Canadell JG, Sitch S and others (2016) Global carbon budget 2016. Earth Syst Sci Data 8: 605–649

Leu E, Daase M, Schulz KG, Stuhr A, Riebesell U (2013) Effect of ocean acidification on the fatty acid composition of a natural plankton community. Biogeosciences 10: 1143–1153

Löder MG, Meunier C, Wiltshire KH, Boersma M, Aberle N (2011) The role of ciliates, heterotrophic dinoflagellates and copepods in structuring spring plankton communities at Helgoland Roads, North Sea. Mar Biol 158: 1551–1580

Lohbeck KT, Riebesell U, Reusch TB (2012) Adaptive evolution of a key phytoplankton species to ocean acidification. Nat Geosci 5:346–351

Lyngsgaard MM, Richardson K, Markager S, Nielsen MH, Oelsen M, Christensen JPA (2014) Deep primary production in coastal pelagic systems: importance for ecosystem functioning. Mar Ecol Prog Ser 517:15–33

Malzahn A, Aberle N, Clemmesen C, Boersma M (2007) Nutrient limitation of primary producers affects planktivorous fish condition. Limnol Oceanogr 52:2062–2071

Malzahn AM, Hantzsche F, Schoo KL, Boersma M, Aberle N (2010) Differential effects of nutrient-limited primary production on primary, secondary or tertiary consumers. Oecologia 162:35–48

Melzner F, Thomsen J, Koeve W, Oschlies A and others (2013) Future ocean acidification will be amplified by hypoxia in coastal habitats. Mar Biol 160:1875–1888

Menden-Deuer S, Lessard EJ (2000) Carbon to volume relationships for dinoflagellates, diatoms, and other protist plankton. Limnol Oceanogr 45:569–579

Meyer J, Riebesell U (2015) Reviews and syntheses: responses of coccolithophores to ocean acidification: a meta-analysis. Biogeosciences 12:1671–1682

Molvær J, Eikrem W, Magnusson J, Pedersen A, Tjomsland T (2007) The OSPAR comprehensive procedure for the Norwegian west coast—eutrophication status. Norwegian Institute for Water Research, Oslo

Müller-Navarra DC, Brett MT, Liston AM, Goldman CR (2000) A highly unsaturated fatty acid predicts carbon transfer between primary production and consumers. Nature 403:74–77

Nielsen TG (1991) Contribution of zooplankton grazing to the decline of a *Ceratium* bloom. Limnol Oceanogr 36: 1091–1106

Oksanen J (2011) Vegan: community ecology package. R package ver. 2.0-2. http://CRAN.R-project.org/package=vegan

Olenina I, Hajdu S, Edler L, Wasmund N and others (2006) Biovolumes and size-classes of phytoplankton in the Baltic Sea. HELCOM Baltic Sea Environmental Proceedings No. 106. Helsinki Commission Baltic Marine Environment Protection Commission, Helsinki

Pankow H (1990) Ostsee-Algenflora. Fischer, Jena

Pedersen MF, Hansen PJ (2003) Effects of high pH on the growth and survival of 6 marine heterotrophic protists. Mar Ecol Prog Ser 260:33–41

Pinheiro J, Bates D, DebRoy S, Sarkar D, R Core Team (2020) nlme: linear and nonlinear Mixed Effects Models. R package version 3.1-148. https://CRAN.R-project.org/package=nlme

Putt M, Stoecker DK (1989) An experimentally determined carbon:volume ratio for marine oligotrichous ciliates from estuarine and coastal waters. Limnol Oceanogr 34: 1097–1103

R Core Team (2017) R: a language and environment for statistical computing. R Foundation for Statistical Computing, Vienna

Rahmstorf S, Coumou D (2011) Increase of extreme events in a warming world. Proc Natl Acad Sci USA 108:17905–17909

Riebesell U, Revill AT, Holdsworth DG, Volkman JK (2000) The effects of varying CO_2 concentration on lipid composition and carbon isotope fractionation in *Emiliania huxleyi*. Geochim Cosmochim Acta 64:4179–4192

Riebesell U, Schulz KG, Bellerby RGJ, Botros M and others (2007) Enhanced biological carbon consumption in a high CO_2 ocean. Nature 450:545–548

Riebesell U, Czerny J, von Bröckel K, Boxhammer T and others (2013) Technical note: a mobile sea-going mesocosm system — new opportunities for ocean change research. Biogeosciences 10:1835–1847

Riebesell U, Bach LT, Bellerby RGJ, Bermúdez R and others (2017) Ocean acidification impairs competitive fitness of a predominant pelagic calcifier. Nat Geosci 10:19–24

Riebesell U, Aberle-Malzahn N, Achterberg EP, Algueró-Muñiz M and others (2018) Toxic algal bloom induced by ocean acidification disrupts the pelagic food web. Nat Clim Chang 8:1082–1086

Rossoll D, Bermúdez R, Hauss H, Schulz KG, Riebesell U, Sommer U, Winder M (2012) Ocean acidification-induced food quality deterioration constrains trophic transfer. PLOS ONE 7:e34737

Rost B, Richter KU, Riebesell U, Hansen PJ (2006) Inorganic carbon acquisition in red tide dinoflagellates. Plant Cell Environ 29:810–822

Sala MM, Aparicio FL, Balague V, Boras JA and others (2016) Contrasting effects of ocean acidification on the microbial food web under different trophic conditions. ICES J Mar Sci 73:670–679

Sarkar D (2008) Lattice: multivariate data visualization with R. Springer, New York, NY. http://lmdvr.r-forge.r-project.org

Sargent JR, Falk-Petersen S (1988) The lipid biochemistry of calanoid copepods. Hydrobiologia 167:101–114

Schulz KG, Bellerby RGJ, Brussaard CPD, Büdenbender J and others (2013) Temporal biomass dynamics of an Arctic plankton bloom in response to increasing levels of atmospheric carbon dioxide. Biogeosciences 10:161–180

Schulz KG, Bach LT, Bellerby RGJ, Bermúdez R and others (2017) Phytoplankton blooms at increasing levels of atmospheric carbon dioxide: experimental evidence for negative effects on prymnesiophytes and positive on small picoeukaryotes. Front Mar Sci 4:64

Skovgaard A (1996) Engulfment of *Ceratium* spp. (Dinophyceae) by the thecate photosynthetic dinoflagellate *Fragilidium subglobosum*. Phycologia 35:490–499

Smetacek V (1981) Annual cycle of protozooplankton in the Kiel Bight. Mar Biol 63:1–11

Smetacek V, Hendrikson P (1979) Composition of particulate organic matter in Kiel Bight in relation to phytoplankton succession. Oceanol Acta 2:287–298

Sommer U, Paul C, Moustaka-Gouni M (2015) Warming and ocean acidification effects on phytoplankton — from species shifts to size shifts within species in a mesocosm experiment. PLOS ONE 10:e0125239

Spisla C, Bach LT, Taucher J, Boxhammer T, Yong JC (2020) KOSMOS Bergen 2015 mesocosm study: environmental data, carbonate chemistry and nutrients.

Støttrup JG, Jensen J (1990) Influence of algal diet on feeding and egg production of the calanoid copepod *Acartia tonsa* Dana. J Exp Mar Biol Ecol 141:87–105

Suffrian K, Simonelli P, Nejstgaard J, Putzeys S, Carotenuto Y, Antia A (2008) Microzooplankton grazing and phytoplankton growth in marine mesocosms with increased CO_2 levels. Biogeosciences 5:1145–1156

Taguchi S (1981) Seasonal studies of the dinoflagellate *Ceratium longipes* (Bailey) Gran in the Bedford Basin, Canada. J Exp Mar Biol Ecol 55:115–131

Tang Y, Horikoshi M, Li W (2016) "ggfortify: unified interface to visualize tatistical result of popular R packages." The R Journal, 8. https://journal.r-project.org/

Tatters AO, Roleda MY, Schnetzer A, Fu F and others (2013) Short- and long-term conditioning of a temperate marine diatom community to acidification and warming. Philos Trans R Soc B 368:20120437

Taucher J, Haunost M, Boxhammer T, Bach L, Alguer Muiz MA, Riebesell U (2017) Influence of ocean acidification on plankton community structure during a winter-to-summer succession: an imaging approach indicates that copepods can benefit from elevated CO_2 via indirect food web effects. PLOS ONE 12:e0169737

Tortell PD, Payne CD, Li Y, Trimborn S and others (2008) CO_2 sensitivity of Southern Ocean phytoplankton. Geophys Res Lett 35:L04605

Trimborn S, Brenneis T, Sweet E, Rost B (2013) Sensitivity of Antarctic phytoplankton species to ocean acidification: growth, carbon acquisition, and species interaction. Limnol Oceanogr 58:997–1007

Tsuzuki M, Ohnuma E, Sato N, Takaku T, Kawaguchi A (1990) Effects of CO_2 concentration during growth on fatty acid composition in microalgae. Plant Physiol 93:851–856

Utermöhl H (1958) Zur Vervollkommnung der quantitativen Phytoplankton-Methodik. Mitt Int Ver Theor Angew Limnol 9:1–38

Wynn-Edwards C, King R, Davidson A, Wright S and others (2014) Species-specific variations in the nutritional quality of southern ocean phytoplankton in response to elevated pCO_2. Water (Basel) 6:1840–1859

Editorial responsibility: Toshi Nagata, Kashiwanoha, Japan

Submitted: September 24, 2019; Accepted: June 12, 2020
Proofs received from author(s): August 5, 2020